Defect Characterization in SiGe/SOI Epitaxial Semiconductors by Positron Annihilation

R. Ferragut · A. Calloni · A. Dupasquier ·
G. Isella

Abstract The potential of positron annihilation spectroscopy (PAS) for defect characterization at the atomic scale in semiconductors has been demonstrated in thin multilayer structures of SiGe (50 nm) grown on UTB (ultra-thin body) SOI (silicon-on-insulator). A slow positron beam was used to probe the defect profile. The SiO_2/Si interface in the UTB-SOI was well characterized, and a good estimation of its depth has been obtained. The chemical analysis indicates that the interface does not contain defects, but only strongly localized charged centers. In order to promote the relaxation, the samples have been submitted to a post-growth annealing treatment in vacuum. After this treatment, it was possible to observe the modifications of the defect structure of the relaxed film. Chemical analysis of the SiGe layers suggests a prevalent trapping site surrounded by germanium atoms, presumably Si vacancies associated with misfit dislocations and threading dislocations in the SiGe films.

Keywords Positron annihilation spectroscopy · Ultra-thin body films · SiGe semiconductors · Point defects

Introduction

Silicon–germanium (SiGe) has gained much attention in recent years thanks to its promising electrical and material properties. The complete solubility of the two elements enables band gap engineering, and SiGe is relatively easy to integrate into silicon technology. There are, however, still numerous issues regarding the electrical and material properties of SiGe that have to be clarified, e.g. the formation of electrically active defect complexes such as vacancy-type defects.

The positron annihilation technique is an established method for investigating point defects in materials [1]. When a positron is implanted into condensed matter, it annihilates with an electron and emits two 511 keV γ-rays. The energy spectrum of the annihilation γ-rays is broadened due to the Doppler effect associated with the momentum component of the annihilating electron–positron pair. Positrons tend to be localized in vacancy-type defects because of the Coulomb repulsion from ion cores. Since the momentum distribution of electrons in such defects differs from that in bulk materials, one can detect the defects by measuring the Doppler-broadening spectra of annihilation radiation. A frequently adopted parameter used for characterizing the change in the Doppler-broadening spectra is the so-called S parameter, which mainly reflects changes in the low-momentum region of the electron momentum distribution [1].

Previous investigations comprise the study of semiconductor layers (usually in the range of hundreds of nanometers) and semiconductor/oxide systems. The present contribution deals with positron implantation into UTB-SOI (ultra-thin body-silicon-on-insulator) and SiGe/SOI multilayer structures (partially presented in Ref. 2). The position and chemical environment of the SiO_2/Si interface in the UTB-SOI was well characterized. SiGe/SOI have been proposed as an efficient way of producing strain-free substrates by strain equalization between the top crystalline layers or by strain transfer to the buried oxide [3, 4]. Chemical analysis of the annihilation site in the SiGe films suggests a prevalent decoration of the trapping sites (vacancy-like defects) with Ge atoms associated with misfit

R. Ferragut (✉) · A. Calloni · A. Dupasquier · G. Isella
L-NESS, Dipartimento di Fisica, Politecnico di Milano,
via Anzani 42, 22100 Como, Italy
e-mail: rafael.ferragut@polimi.it

dislocations and threading dislocations. The capabilities of PAS include the identification and analysis of different type of defects in epitaxial SiGe thin films and the UTB-SOI substrate in a nondestructive manner.

Experimental Method

The UTB-SOI wafers, purchased from SOITEC[TM], were prepared according to the SmartCut[TM] process, based on implantation and wafer bonding [5]. All the SOI wafers used have a (100) crystal orientation and are slightly p-doped (Boron $0.6-1.6 \times 10^{15}$ cm^{-3}), as was the Si reference sample.

The SiGe layers were grown on SOI by means of LEPECVD (low-energy plasma-enhanced chemical vapor deposition) [6]. The SOI samples were heated to a temperature of 500°C for 136 s during SiGe growth. The SiGe layers were grown with a 36% germanium atomic concentration (measured by X-ray diffraction). In order to promote relaxation, the samples have been submitted to a post-growth annealing treatment in vacuum ($\sim 10^{-5}$ mbar). SiGe layer and silicon substrate thickness were optimized in order to give a substantial relative change (from 18 to 56%) of the degree of relaxation (normalized difference between the measured lattice parameter and the strain-free lattice parameter dependent on the germanium concentration) upon the annealing treatment. Investigated samples are listed in Table 1.

The measurement was performed by means of a slow positron beam, capable of implanting positrons with a kinetic energy variable from 0.05 to 18 keV. The mean positron implantation depth Z_m depends on E according to the formula

$$Z_m = \frac{40}{\rho} E^{1.6}, \qquad (1)$$

with Z_m in nanometers when density ρ and positron implantation energy E are expressed in grams per cubic centimeter and keV, respectively [7].

The gamma rays produced by positron annihilation were detected by means of a high purity germanium detector with resolution (FWHM) of about 1.32 keV at 511 keV. For each implantation energy, approximately 10^5 counts

Table 1 Characteristics of the samples used in current measurements

Sample	Structure[a]	Thermal treatment
SOI	2 Si/147 SiO$_2$/Si	As-received
SiGe (a)	50 Si$_{0.64}$Ge$_{0.36}$/10 Si/147 SiO$_2$/Si	As-grown
SiGe (b)	50 Si$_{0.64}$Ge$_{0.36}$/10 Si/147 SiO$_2$/Si	33 min at 750°C

[a] Thicknesses are given in nanometers. All samples were covered by a thin layer of natural oxide (~ 2 nm)

were accumulated in the annihilation peak. Measurements were taken in high vacuum conditions, $\sim 10^{-9}$ mbar. The annihilation energy spectra have been analyzed both by extracting the full annihilation peak shape and by integrating the annihilation peak in the energy interval $|E-511 \text{ keV}| \leq 0.85$ keV (S parameter). The area under the peak ($|E-511 \text{ keV}| \leq 4.25$ keV) was used for normalization. Since the energy of the annihilation radiation is Doppler shifted in the laboratory frame as a consequence of a finite momentum of the positron–electron annihilating pair along the line that connects the sample to the gamma ray detector, the annihilation peak changes its shape according to the momentum distribution of the electron cloud seen by the positron. An increase of the S parameter thus reflects an increased annihilation rate with free (i.e. valence) electrons, while a broadening of the peak can be linked to an enhanced interaction rate with more bound (i.e. core) electrons.
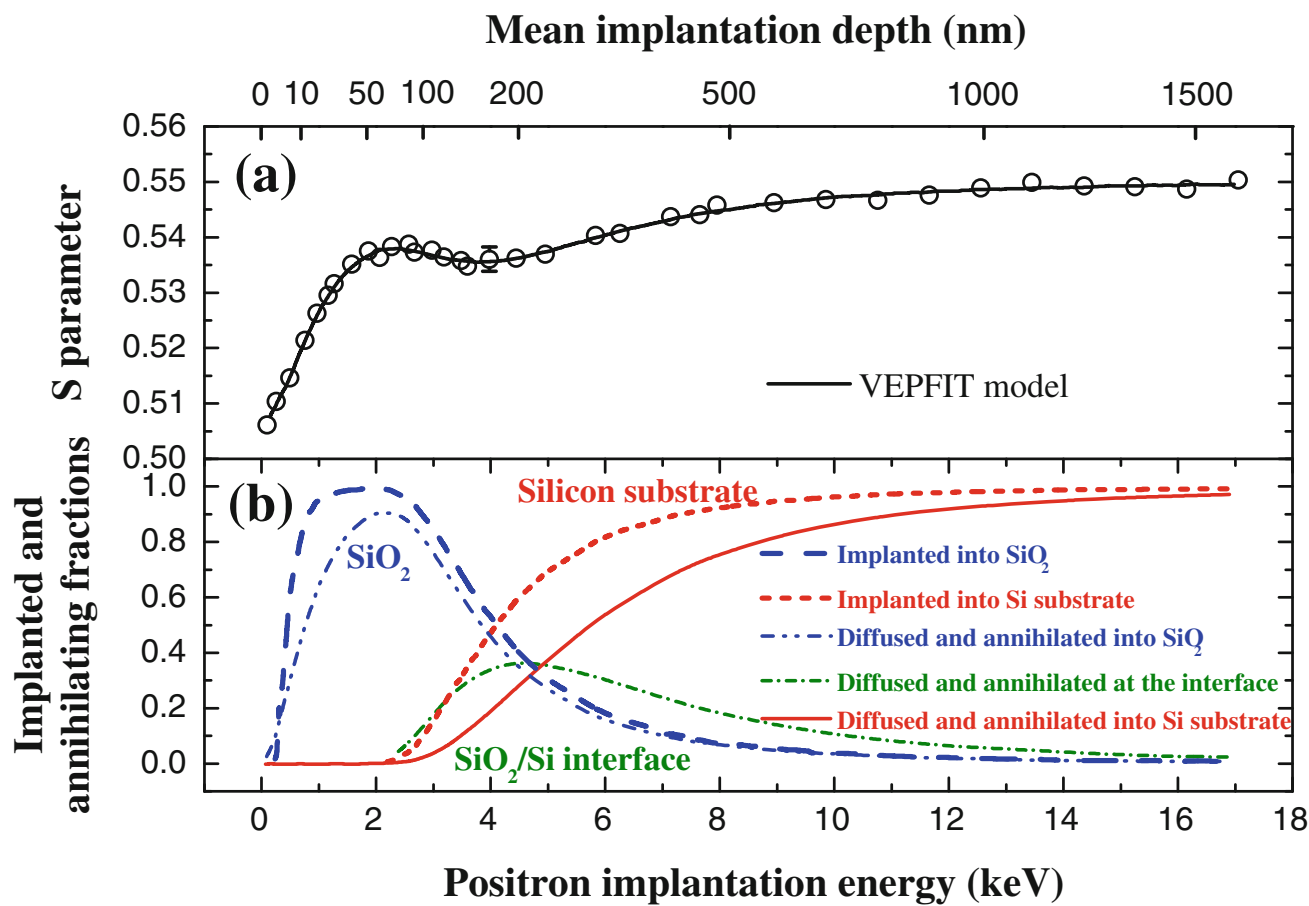
Results and Discussion

Figure 1 shows the results of positron implantation into a bare SOI substrate with an extremely thin (~ 2 nm) Si layer on top. The S parameter evolution with the implantation energy is shown in panel a, while panel b shows the fraction of positrons annihilated into the oxide, the substrate, and into the buried interface as computed by the application of a positron implantation and diffusion algorithm by means of the VEPFIT program [8]. Although positrons are not directly implanted at interfaces, a substantial fraction of positrons should annihilate into the buried interface at implantation energies higher than 2 keV. The evident dip in the S parameter curve at about 3.5 keV is certainly related to strong positron trapping at interface. This is confirmed by the excellent fit of the experimental data with the VEPFIT model (solid line in Fig. 1a). This line is the outcome of several attempts with different models (sets of VEPFIT input data), which in all cases imply the presence of a positron trapping region corresponding to the nominal position of the Si/SiO$_2$ interface. The VEPFIT curve in Fig. 1a was obtained by assuming an oxide surface and four more layers: Si, SiO$_2$, SiO$_2$/Si interface, and a semi-infinite Si layer. The corresponding best-fit values of positron diffusion lengths L_+, thicknesses, and S-parameters of the different layers are reported in Table 2. It was necessary to fix some parameters (labeled F in Table 2). In accordance with Refs. [9] and [10], the interface was modeled as a very thin layer (1 nm) with a short positron diffusion length ($L_+ \sim 1$ nm). The best-fit value of the depth of the interface coincides within the experimental error with the nominal value. The introduction of an electric field near the interface region is

Fig. 1 a S parameter as a function of the positron implantation energy in the SOI sample. *Error bar* is shown for one point only. **b** *Dashed lines* represent the fractions of positrons implanted into the oxide (*blue*) and the silicon substrate (*red*), calculated according to Ref. [11]. The *continue* and *dash-doted lines* represent the fractions of positrons that annihilate after diffusion in the oxide (*blue*), at the buried interface (*green*) and into the substrate (*red*). Surface effects are not visible in the picture (important only at low energies). The *upper scale* gives the mean positron implantation depth calculated according to Eq. 1

also possible (~ 300 V/cm), but in this case, it is necessary to fix the interface position at the nominal value (147 nm). Attempts to introduce another absorbing layer at the first Si/SiO$_2$ interface seem arbitrary.

Figure 2 shows the ratio of the positron–electron annihilation peaks of the surface, the SiO$_2$ layer, and the SiO$_2$/Si interface relative to the bulk silicon peak. The surface and interface signals were obtained by means of a

linear combination between the oxide, the interface, and a silicon bulk contributions, with the weights given by the fractions shown in Fig. 1b. Since both the positron

Table 2 Results obtained in the Si/SiO$_2$/Si SOI heterostructure from the positron lineshape profile (Fig. 1) using VEPFIT

|	L_+ (nm)	t (nm)	S parameter
Surface	<1	~2F	0.508 ± 0.003
Si	220F	2F	0.551F
SiO$_2$	17 ± 4	149 ± 3	0.541 ± 0.002
SiO$_2$/Si interface	~1F	~1F	0.525 ± 0.004
Si	220 ± 20	∞	0.551 ± 0.001

Positron diffusion length L_+, thickness t, and Doppler S parameter. Fixed parameters are marked with the letter F
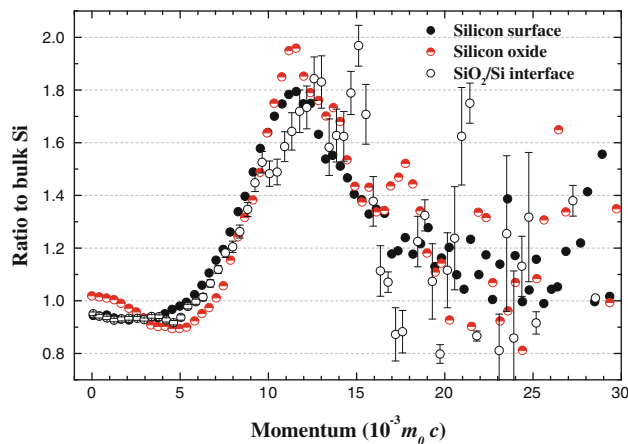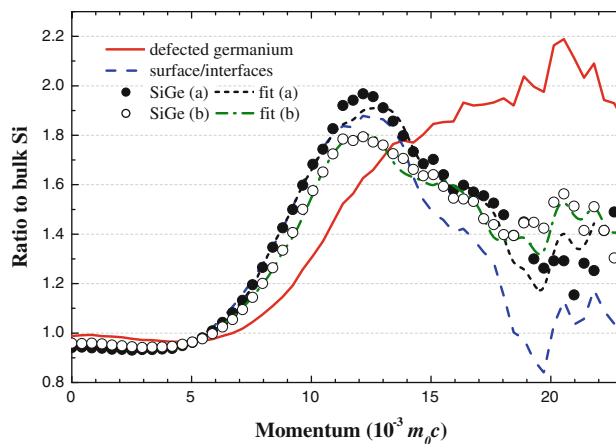

Fig. 2 Ratios of the positron–electron momentum distribution at the surface of a silicon reference sample, in the silicon oxide and at the buried interface (relative to bulk Si)

diffusion coefficient and the lineshape parameters relative to the thermally grown oxide and to the silicon substrate are known from the literature and from calibration experiments on bulk samples [12], the interface Doppler peak shape can be extracted. The interface peak of the Doppler ratio curve of Fig. 2 is characterized by a flat region at low momentum and by a peak at ~12 mrad ($12 \times 10^{-3}\ m_0\ c$) due to annihilation with tightly bound oxide electrons. The absence of a clear signal of an increment of annihilation with nearly free electrons (visible at momentum zero in Fig. 2) and the need of a trapping layer at the interface convey the idea that positrons do not annihilate into voids, but rather that they are strongly localized at charged centers, most probably representing electron states created by the presence of silicon dangling bonds [13, 14], as already demonstrated in positron implantation experiments with SiO_2/Si samples [7] and that they sense a relatively well-ordered oxide structure, typical of low quartz [15]. The same annihilation environment can be found more or less at any semiconductor surface covered with thermally grown or natural oxide, as seen in Fig. 2.

Figure 3 shows the experimental S parameter profiles of the SiGe/SOI samples listed in Table 1. The approximated mean implantation depth was calculated according to Eq. 1 (the density of the SiGe layer has been estimated to be 3.52 g/cm^3). The results indicate the existence of a wide plateau up to ~50 nm in both samples, which corresponds to the SiGe layer, and changes in height appear after the thermal treatment. Given the mixing between the signals coming from the oxide and from the SiGe/Si layers, changes in the surface layers morphology can be appreciated by comparing the two S parameter evolutions relative to the sample before and after structural relaxation due to the annealing step. The increase of the S parameter at low
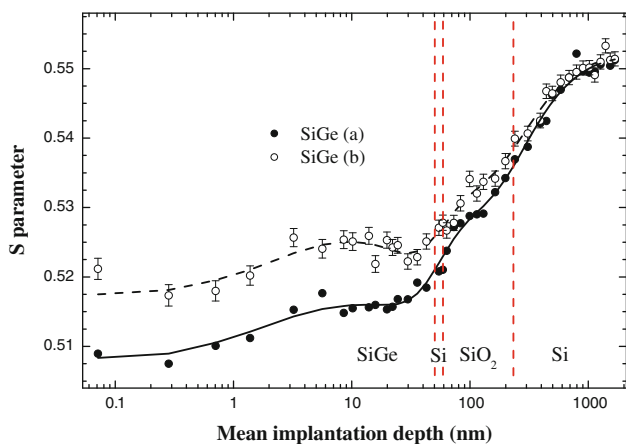
Fig. 4 Ratios of the positron–electron momentum distribution of the annihilating pair in SiGe **a** "as grown" (full symbols) and SiGe **b** annealed (open symbols) relative to bulk Si. Linear combination fits for **a** "as grow" (short dashed line) and **b** annealed (dot-dashed line). The reference spectra of defected Ge and surface/interface are shown with continue and dashed lines (after Ref. [2])

implantation energy can be thus directly related to an enhanced interaction with free electrons. The exact positioning of the defected region is behind the resolution limits of the current measurements, given that the positron diffusion length in intrinsic semiconductors can be as high as 240 nm [12].

In order to gain more understanding on the environment of the positron annihilation site, we have averaged the Doppler peak shape relative to a mean implantation depth between 2 and 30 nm (the plateaus in Fig. 3). Lower implantation energies have been neglected since they bring information also from the annihilation of positron from non-thermalised ensemble and from the natural oxide layer. According to both precise VEPFIT simulations and to simplified models of positron implantation, positrons implanted at energies lower than 2 keV annihilate almost exclusively in the topmost SiGe/Si layers. Since the diffusion length of positrons into bulk semiconductors exceeds the actual thickness of these layers, the annihilation peak shape prevalently resembles the one characteristic of annihilation at the oxide/semiconductor interface. The differences between the peak shape relative to the as-grown sample and to the annealed one are shown in Fig. 4 and are related to an increased annihilation with low- and high-momentum electrons. The former effect is reflected in the increase of the S parameter, as seen in Fig. 3 and can be associated with an increase of positron annihilation at defects, and the latter can be interpreted as a modification of the chemical environment of the positron annihilation site.

The chemical sensitivity of positrons has been demonstrated in metals and semiconductor systems [16, 17].

Fig. 3 S parameter as a function of the mean implantation depth: SiGe **a** "as grown" (full symbols); SiGe **b** annealed (open symbols). Continuous and dashes lines are VEPFIT simulations, while vertical dashed lines mark the position of interfaces (after Ref. [2])

Following the procedure outlined in [18], we have reproduced the measured annihilation peak shapes with a linear combination of Doppler spectra of the semiconductor/oxide interface and the Ge signal of a sample saturated of defects. The obtained fits are shown in Fig. 4. As discussed in Ref. [2], the results of this latter analysis to the data of Fig. 4 show an increment in the germanium component from $(22 \pm 10)\%$ to $(47 \pm 8)\%$ after the annealing. The indetermination of this component is associated with the spread of the experimental data, especially at high momentum. In particular, in order to better reproduce the measured Doppler spectra on the whole momentum scale, we have employed, instead of the annihilation peak shape characteristics of annihilation into bulk germanium, the shape measured from a thick (in the microns range) layer of germanium grown on silicon. The abrupt junction between germanium and silicon promotes the formation of misfit dislocations at the interface and threading dislocation that run across the whole germanium layer with an estimated density of about 10^9 cm^{-2}. Positrons are trapped at defect sites causing a substantial reduction of the diffusion length and a slight increase of the S parameter. This experimental finding can be explained by postulating positron annihilation at vacancies associated with dislocations, or at negatively charged centers associated with dislocations, given that the deposited Ge layer was free of contaminants or dopant atoms, which are known to produce positron trapping defects [1]. The decomposition of the annihilation spectra into two terms (interface and "germanium defects") gives an acceptable fit (χ^2/[degrees of freedom] values of 1.5 in the as-grown sample and 1.2 in the annealed sample) and conveys the idea of a prevalent decoration of positron trapping centers with germanium atoms (as already pointed out by Rummukainen et al. [19] in bulk SiGe layers), mainly associated with Si vacancies.

Conclusions

This work presents the characterization of SOI and SiGe/SOI samples.

(i) The SiO$_2$/Si interface in the UTB-SOI was identified with accuracy. It was possible to estimate the depth where the interface is located with good precision. The chemical analysis at the surface and the interface shows that positrons do not annihilate into large defects (voids), but rather that they are strongly localized close to the silicon surface. The observed momentum distribution is characteristic of annihilation in a relatively well-ordered oxide structure, typical of low quartz [15], and the strong localization

can be explained with annihilation at negatively charged centers, like silicon dangling bonds [7, 14].

(ii) The process of strain relaxation in thin SiGe layers grown on SOI substrates has been analyzed. Relaxation of the strained structure has been found to proceed via the introduction of new defects, presumably Si vacancies, able to trap positrons. Chemical analysis of the annihilation site suggests a prevalent decoration of the trapping sites with germanium atoms. The formation of lattice defects in the form of misfit dislocations between two adjacent layers and threading dislocations in the SiGe substrate are certainly associated with the identified defects.

It is demonstrated that the analysis of positron data coming from extremely thin surface layers is possible thanks to the reduced implantation range of positrons at low implantation energy and to the enhanced contrast due to the prevalent annihilation of not trapped positrons with strongly bound surface/interface oxide electrons.

References

1. R. Krause-Rehberg, H. Leipner, *Positron Annihilation in Semiconductors* (Springer, Berlin, 1999)
2. A. Calloni, R. Ferragut, F. Moia, A. Dupasquier, G. Isella, D. Marongiu, G. Norga, A. Federov, D. Chrastina, Phys. Stat. Sol. (C) **6**, 2304 (2009)
3. A.R. Powell, Appl. Phys. Lett. **64**, 1586 (1994)
4. F.K. LeGoues, A. Powell, S.S. Iyer, J. Appl. Phys. **75**, 7240 (1994)
5. M. Bruel, Nucl. Instr. Meth. B **108**, 313 (1996)
6. C. Rosenblad, H.R. Deller, M. Döbeli, E. Müller, H. von Känel, Thin Solid Films **318**, 11 (1998)
7. P. Asoka-Kumar, K.G. Lynn, D.O. Welch, J. Appl. Phys. **76**, 4935 (1994)
8. A. van Veen, H. Schut, J. de Vries, R.A. Hakvoort, M.R. Ijpma, AIP Conf. Proc. **218**, 171 (1990)
9. A. Uedono, L. Wei, S. Tanigawa, R. Suzuki, H. Ohgaki, T. Mikado, K. Fujino, J. Appl. Phys. **75**, 216 (1994)
10. R.S. Brusa, G.P. Karwasz, G. Mariotto, A. Zecca, R. Ferragut, P. Folegati, A. Dupasquier, G. Ottaviani, R. Tonini, J. Appl. Phys. **94**, 7483 (2003)
11. A. Vehanen, K. Saarinen, P. Hautojärvi, H. Huomo, Phys. Rev. B **35**, 4606 (1987)
12. P.J. Schultz, K.G. Lynn, Rev. Mod. Phys. **60**, 701 (1988)
13. M.H. White, J.R. Cricchi, IEEE Trans. Electron Dev. **19**, 1280 (1972)
14. S.M. Sze, K. Kwok, *Ng, Physics of Semiconductor Devices*, 3rd edn. (Wiley, New Jersey, 2007)

15. G. Brauer, W. Anwand, W. Skorupa, A.G. Revesz, J. Kuriplach, Phys. Rev. B **66**, 195331 (2002)
16. S. Szpala, P. Asoka-Kumar, B. Nielsen, J.P. Peng, S. Hayakawa, K.G. Lynn, H.-J. Gossmann, Phys. Rev. B **54**, 4722 (1996)
17. A. Dupasquier, R. Ferragut, M.M. Iglesias, M. Massazza, G. Riontino, P. Mengucci, G. Barucca, C.E. Macchi, A. Somoza, Phil. Mag. **87**, 3297 (2007)
18. P. Folegati, I. Makkonen, R. Ferragut, M.J. Puska, Phys. Rev. B **75**, 054201 (2007)
19. M. Rummukainen, J. Slotte, K. Saarinen, H.H. Radamson, J. Hallstedt, A.Yu. Kuznetsov, Phys. Rev. B **73**, 165209 (2006)